Transport optimization in stellarators

Cite as: Phys. Plasmas **13**, 058102 (2006); https://doi.org/10.1063/1.2177643
Submitted: 28 October 2005 . Accepted: 27 December 2005 . Published Online: 08 May 2006

H. E. Mynick

Transport optimization in stellarators[a)]

H. E. Mynick[b)]
Plasma Physics Laboratory, Princeton University, P.O. Box 451, Princeton, New Jersey 08543-0451

(Received 28 October 2005; accepted 27 December 2005; published online 8 May 2006)

A survey of the approaches which have been developed for mitigating transport in stellarators is presented. A primary deficiency of stellarators has been elevated transport levels due to their nonaxisymmetry. Since the early 1980s, stellarator research has addressed this difficulty, developing a range of techniques for reducing transport, both neoclassical and, more recently, also anomalous. Several of these approaches are now being implemented in a new generation of experiments in the United States and abroad. This paper describes the fundamental physics of these methods for transport reduction. © *2006 American Institute of Physics*. [DOI: 10.1063/1.2177643]

I. INTRODUCTION

Stellarators have much in common with tokamaks, and some attractive features relative to them—disruption-free performance, and no requirement for current drive to produce a rotational transform. However, a major drawback has been elevated levels of neoclassical transport due to their nonaxisymmetry. Beginning in the early 1980s, stellarator research has addressed this deficiency, developing a range of approaches for stellarator "transport-optimization," i.e., for mitigating stellarator transport, both neoclassical and, more recently, also anomalous transport. Several of these techniques for transport optimization are now being implemented in a new generation of experiments in the United States and abroad.[1–5] In this paper, we review the basic physics of these transport optimization approaches.

In Sec. II we begin by introducing some useful notation, and discuss the range of stellarators which exist, both in theory, and increasingly, in experimental implementation. These devices share features of their particle orbits and neoclassical transport, and in Sec. III, we present an overview of these, to clarify the mechanisms producing the undesirable enhanced transport levels. In Sec. IV, we then address the various approaches which have been developed to mitigate this transport, and in Sec. V we discuss methods more recently being uncovered to also reduce turbulent transport. A summarizing discussion is given in Sec. VI.

II. PRELIMINARIES

Like a tokamak, a stellarator is a toroidal confinement device, with nested flux surfaces and rotational transform $\iota \equiv q^{-1}$. It is convenient to parametrize these toroidal devices with a coordinate system natural to the magnetic geometry, viz., with flux (or magnetic) coordinates (ψ, θ, ζ). Here, $2\pi\psi$ is the toroidal flux within a flux surface, and with the pair of poloidal and toroidal angles (θ, ζ) chosen so that the magnetic field can be written in the Clebsch (contravariant) form $\mathbf{B}=\nabla\psi\times\nabla\theta+\nabla\zeta\times\nabla\psi_p=\nabla\psi\times\nabla\alpha_p$, with $2\pi\psi_p$ the poloidal flux, Clebsch angle $\alpha_p \equiv \theta-\iota\zeta$, constant along a field line, and $\iota \equiv d\psi_p/d\psi$. It is also useful to define an average minor radius $r(\psi)$ with units of length by $\psi \equiv \bar{B}_x r^2/2$, with $B_x(\zeta)$ the magnetic field strength on axis (denoted by the subscript x), and $\bar{B}_x$ its average.

An important property of the guiding-center equations of motion in flux coordinates is that they depend only on the magnitude $B \equiv |\mathbf{B}|$ of the magnetic field, and not on its individual components,[6] giving it a central role in determining the particle orbits in these coordinates. B may be written as a Fourier decomposition $B(\mathbf{x})=\Sigma_{m,n}B_{mn}(r)\cos(n\zeta-m\theta)$, and for purposes of analysis modeled by

$$B(\mathbf{x}) = \bar{B}(r)[1 - \delta_t(r,\theta) - \delta_h(\mathbf{x})\cos\,\eta], \tag{1}$$

with $\bar{B}(r) \equiv \langle B(\mathbf{x})\rangle = B_{00}(r)$ the flux-surface average of B. The axisymmetric $(n=0)$ portion of this is given by the $1-\delta_t$ terms, with $\delta_t \equiv \varepsilon_t(r)c(\theta)=\Sigma_{m\neq 0}(B_{m0}/\bar{B})\cos m\theta$, toroidal amplitude $\varepsilon_t(r)$, and $c(\theta)$ generalizing the $\cos(\theta)$ dependence in a circular tokamak, in which case ε_t is the inverse aspect ratio r/R_0. One notes from this that $\langle\delta_t\rangle=0=\langle c(\theta)\rangle$. Further requiring that, as for $\cos\theta$, $c(\theta=0)=1$ fully specifies these quantities, with $\varepsilon_t=\Sigma_{m\neq 0}(B_{m0}/\bar{B})$. The nonaxisymmetric portion is represented by the term $\delta_h\cos\eta$, with ripple amplitude $\delta_h \equiv \varepsilon_h(r)k(\mathbf{x})$ having flux-surface average $\varepsilon_h(r)$, and modulating factor $k(\mathbf{x})$, allowed to vary slowly over a flux surface. $\eta \equiv n\zeta - m\theta$ is the single ripple phase. While this nonaxisymmetric term is not fully general, it captures the features of most stellarators of interest, including those discussed here. In fact, most of analytic stellarator neoclassical (nc) theory was developed using the more specialized case $k(\mathbf{x})=1$ of no ripple modulation, i.e., $\delta_h=\langle\delta_h\rangle=\varepsilon_h(r)$.

Because of their 3D character, there are many more different types of stellarators than tokamaks. The essential features of the shape of existing tokamaks may be described by a handful (~ 5) of shape parameters, including the aspect ratio $A \equiv R_0/a_0$, the ellipticity, and triangularity. (Here, R_0 is the major radius of the magnetic axis, and a_0 the minor radius on the midplane.) For stellarators, numerical optimizers which have been used to design recent experiments have typically used several tens of shape parameters. In Fig. 1 a small illustrative sample of six configurations of interest is

[a)]Paper CI1a 1, Bull. Am. Phys. Soc. **50**, 63 (2005).
[b)]Invited speaker.

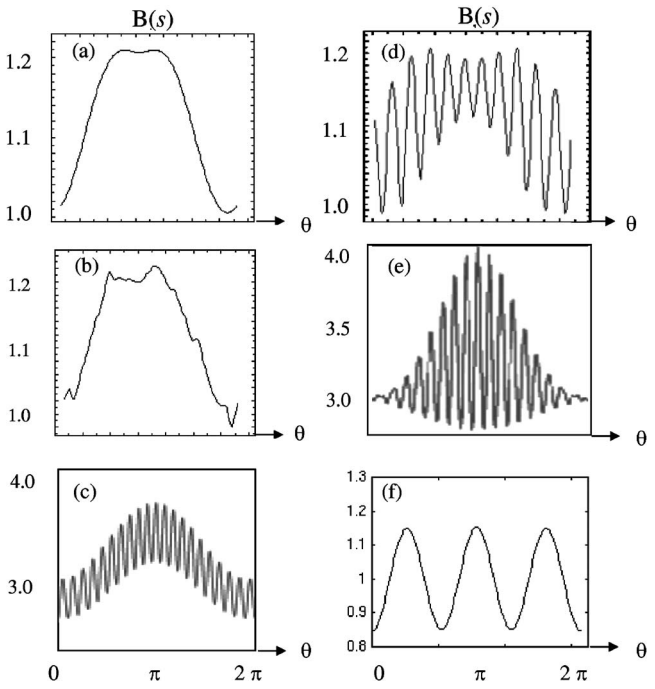

FIG. 1. Profiles of $B(\theta)$ along a field line for one poloidal transit, for six toroidal configurations of interest: (a) tokamak, (b) NCSX, a quasi-axisymmetric stellarator, (c) LHD in "standard" configuation (R_0=3.75 m), (d) CNT, (e) LHD in an "inward-shifted" configuation (R_0=3.53 m), (f) HSX, a quasihelical stellarator.

shown, plotting field strength $B(\theta)$ along a field line for one poloidal transit. These are shown in order of increasing value of $p \equiv \varepsilon_h/\varepsilon_t$, a measure of the distance of the configuration from the two symmetric limits $\varepsilon_h=0$ (axisymmetry) and $\varepsilon_t=0$ (helical symmetry). Thus, in Fig. 1(a) is shown a tokamak, having $p=0$. Figure 1(b) shows the $B(\theta)$ profile for the National Compact Stellarator Experiment (NCSX),[4] a quasi-axisymmetric (QA) stellarator now under construction, which has $p \ll 1$. Removing from this all B_{mn} for $n \neq 0$ results in the "equivalent tokamak" for NCSX shown in Fig. 1(a). In Fig. 1(c) is $B(\theta)$ for the large helical device (LHD) (Ref. 1) in its "standard" configuration (R_0=3.75 m), having $\varepsilon_h \sim \varepsilon_t$ and δ_h nearly constant on a flux surface. Most of the stellarator nc theory was developed assuming a $B(\theta)$ profile of this "conventional stellarator" form. In Fig. 1(d) is the profile for the Columbia Non-neutral Torus (CNT) experiment.[7] This configuration is not transport optimized, but is the first in this sequence manifesting an appreciable modulation of δ_h with θ. Still greater modulation is apparent in Fig. 1(e), the profile for LHD in an inward-shifted configuration[8] (R_0=3.53 m), an example of a "quasi-omnigenous" (QO) or "quasi-isodynamic" (QI) configuration, where (as will be discussed) the modulation is central to its good confinement characteristics. The Wendelstein-7X (W7X) experiment,[2] now under construction, and the Quasi-Poloidal Experiment (QPS),[5] now in its final design phase, will be two additional representatives of this class of stellarators. Finally, in Fig. 1(f) is a profile approximating that in the quasihelical (QH) Helically Symmetric Experiment (HSX),[3] which has $p \gg 1$.

III. NEOCLASSICAL TRANSPORT

While there is a wide spectrum of stellarator types, they have in common many features of their particle motion, and of the resultant nc transport. There is a large literature developing the theory of nc transport in toroidal systems. The reader interested in the detailed analytic development of this theory is referred to reviews[9–13] of the subject. Our purpose here is to provide a summary of those results relevant to the issues in the optimization of stellarator transport.

In Fig. 2 is an overview of stellarator nc theory, showing the four basic "branches" which contribute to the transport in a stellarator. There are two symmetric branches (blue and green curves), and two nonsymmetric branches (red and

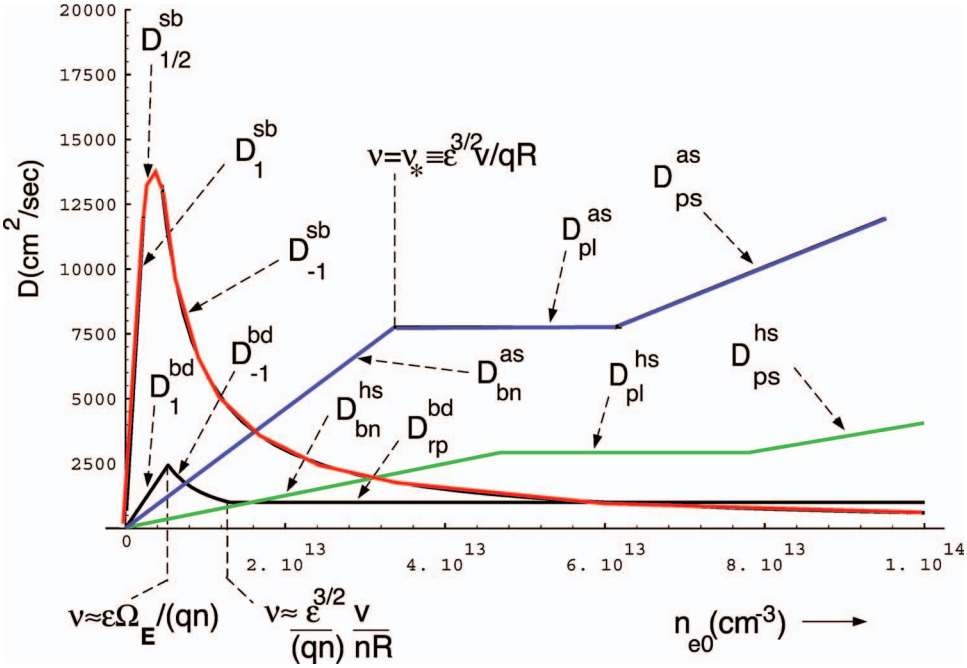

FIG. 2. (Color) Overview of stellarator neoclassical theory, showing the four basic branches contributing to stellarator transport. The superscripts on the transport coefficients D designate the branch (as=axisymmetric, hs=helically symmetric, sb=superbanana, bd=banana drift), subscripts denote the collisionality regime within that branch.

black curves). Plotted is the radial diffusion coefficient D versus central electron density n_{e0}, proportional to collision frequency ν. The branch to which the coefficient belongs is indicated by a superscript, and the particular collisionality regime within that branch is indicated by a subscript.

For an axisymmetric (AS) system ($\varepsilon_h=0$), such as that in Fig. 1(a), only the blue curve (superscript as) is nonvanishing. This is the familiar profile for a tokamak,[9,10] with the banana regime ($D_{\mathrm{bn}}^{\mathrm{as}}$) at its lowest collisionality, turning over into the plateau regime ($D_{\mathrm{pl}}^{\mathrm{as}}$), and the Pfirsch-Schlüter regime ($D_{\mathrm{as}}^{\mathrm{ps}}$) at still higher ν. At low ν, the dominant contributors to transport here are toroidally trapped "bananas," which make a radial drift excursion ("banana-width") ρ_{bt} in the course of a bounce.

The green curve (superscript hs) is the only nonvanishing branch for helically symmetric (HS) systems ($\varepsilon_t=0$), such as that approximated by Fig. 1(f). The dominant low-ν contributors to transport here are ripple-trapped bananas, making drift excursion ρ_{bh}. One notes it has the same form as that for the AS branch, with its own banana, plateau, and Pfirsch-Schlüter regimes.[14] A difference between the two curves, however, is that the HS branch is typically much smaller than the AS one, essentially because ρ_{bt} in a tokamak is large compared to ρ_{bh} in a HS system. This has the notable consequence that transport-optimized stellarators can have nc transport levels much lower than those for a tokamak of the same aspect ratio and rotational transform.

The red curve, dominant at low ν, is the "superbanana" branch (superscript sb). This branch is due to ripple-trapped particles which acquire nonzero bounce-averaged radial drifts $\bar{\dot{r}}$ when ε_t is turned on from a HS system, e.g, when a "straight" stellarator is bent into a torus. (The superbananas are the trajectories traced out by particles which are ripple-trapped over at least some portion of their orbits.)

Finally, the black curve is the "banana-drift" branch (superscript bd).[15–17] In a manner complementary to the sb branch, the principal contributors to this branch are toroidally trapped particles which acquire nonzero bounce-averaged radial drifts $\bar{\dot{r}}$ when an AS system is perturbed, i.e., when ε_h is turned on.

The dominance of the sb branch at low ν is typical for most stellarator parameters, and is thus the principal mechanism which has been addressed by efforts at transport optimization. The bd branch is typically smaller, as in Fig. 2, but can be significant for energetic particles. The sb branch is comprised of two main collisionality regimes, one at very low collisionality ($\nu_h/\Omega_\theta<1$), in which D increases as a positive power of ν,[18,19] and the other valid for $\nu_h/\Omega_\theta>1$, in which D declines as $1/\nu$ (the well-known "$1/\nu$ regime"[20–23]), the two meeting at the peak seen in Fig. 2. Here $\nu_h\equiv\nu/(2\varepsilon_h)$ is the frequency (inverse time) for a particle to collisionally detrap from a ripple well, and $\Omega_\theta=\bar{\dot{\theta}}$ is the poloidal precession frequency, produced by the $E\times B$ and grad B drifts, $\Omega_\theta=\Omega_{\theta E}+\Omega_{\theta B}$, in which $\Omega_{\theta E}\simeq -cE_r/\bar{B}r$ typically dominates for thermal particles. In order of increasing ν, the sb regimes in Fig. 2 are given by $D_1^{\mathrm{sb}}=\sigma_1\nu p(2\varepsilon_h)^{-1/2}v_{Bt}^2/\Omega_\theta^2$, $D_{1/2}^{\mathrm{sb}}=\sigma_{1/2}\nu^{1/2}v_{Bt}^2/\Omega_\theta^{3/2}$, and $D_{-1}^{\mathrm{sb}}=\sigma_{-1}(2\varepsilon_h)^{3/2}v_{Bt}^2/\nu$. with σ_q numerical coefficients obtained from a full kinetic treatment, and $q=1,1/2,-1$ the power of ν appearing in the specified D_q^{sb}.

A superbanana's radial drift has the form $\bar{\dot{r}}\simeq v_{Bt}\sin\theta$, and its poloidal precession $\bar{\dot{\theta}}\simeq\Omega_{\theta E}$ is roughly constant. This results in a collisionless superbanana orbit which is circular in flux coordinates, displaced from a flux surface $r=$const by a "superbanana width" $\Delta_0=v_{Bt}/\Omega_\theta$. Here $v_{Bt}=\varepsilon_t v_{B0}$, with $v_{B0}=\mu\bar{B}/(M\Omega_g r)$, magnetic moment μ, particle mass M, and gyrofrequency Ω_g.

For $\nu_h/\Omega_\theta<1$, the rough form of the collisionless superbanana persists, but collisions perturb the orbit, causing its radial position to wander, analogous to the wandering of bananas for the banana regime. At higher ν ($\nu_h/\Omega_\theta>1$), a particle collisionally detraps after tracing out only a fraction of a full poloidal drift period, making a radial step $\Delta_\nu=v_{Bt}/\nu_h$, resulting in the $1/\nu$ regime.

As described more fully elsewhere,[12,24] the transport coefficients for the D_q^{sb} given above may be obtained by making use of the heuristic formula $D\simeq F\tilde{\nu}\Delta^2$ for diffusion coefficient D, where F is the fraction of particles participating in the random walk process in question, the particles taking radial steps Δ at stepping frequency $\tilde{\nu}$. For example, for the $1/\nu$ regime, F is the fraction $F_h\equiv(2\varepsilon_h)^{1/2}$ of ripple-trapped particles, $\Delta\simeq\Delta_\nu$, and $\tilde{\nu}\simeq\nu_h$. Putting these in the heuristic expression for D yields D_{-1}^{sb}, up to a numerical factor.

The D_q^{sb} above hold for velocity-space shells of particles with constant kinetic energy $W\equiv E-e\Phi$, with Φ the electrostatic potential. To compute the radial particle (heat) flux $\Gamma_s(Q_s)$ for species s, one integrates over W,

$$\begin{bmatrix}\Gamma_s\\ Q_s\end{bmatrix}=-\frac{2n_s}{\sqrt{\pi}}\int dx x^{1/2}e^{-x}\begin{bmatrix}1\\ T_s x\end{bmatrix}D_q(x)\times\left[\frac{n_s'}{n_s}-\frac{e_sE_r}{T_s}+\left(x-\frac{3}{2}\frac{T_s'}{T_s}\right)\right],\tag{2}$$

where $x\equiv W/T_s$. We shall have use for these expressions in Sec. IV B.

IV. OPTIMIZATION OF NEOCLASSICAL TRANSPORT

A list of the approaches which have been developed is given in Table I. Experimental realizations of the concept, either operating or planned, are noted in the right column, in parentheses when the realization was not a fundamental part of the machine design. In this section, we discuss the nc methods, and the turbulent methods in Sec. V. The former list is much more developed, largely because the nc issue has been addressed for far longer than the turbulent one.

The basic objective of nc optimization is to reduce the radial excursion of problematic particles, of which the most troublesome are superbananas, as discussed. Since sb width Δ_0 scales as $\bar{\dot{r}}/\Omega_\theta$, one may hope to reduce Δ_0 either by decreasing $\bar{\dot{r}}$, or by increasing Ω_θ. All of the nc optimization approaches listed in Table I fall into one of these two categories.

TABLE I. Transport optimization methods.

Optimization method	Realization
Neoclassical optimization:	
Reduction of $\bar{\dot{r}}$	
Quasihelical (QH)	HSX
Quasi-axisymmetric (QA)	NCSX
Quasi-poloidal (QP)	QPS
Quasi-omnigenous (QO)/	W7X, (inward-
Quasi-isodynamic (QI)	shifted LHD, CHS)
Isometric/Approx. Omnigenous	⋯
Pseudosymmetric (PS)	⋯
Enhancement of Ω_θ, via ambipolar roots	(CHS, W7AS, LHD, TJ-II)
Enhancement of Ω_θ, magnetic	(W7X at $\beta\sim 0.04$, heliotrons)
Turbulent optimization:	
ITBs via root-jumping	(W7AS, LHD, CHS)
Turbulence modification from shaping	⋯

The grad B and $E\times B$ drifts producing $\bar{\dot{r}}$ and Ω_θ may be written $\mathbf{v}_D=\mathbf{v}_B+\mathbf{v}_E=(\hat{\mathbf{B}}/M\Omega_g)\times\nabla V$, with $V(\mathbf{x})\equiv\mu B+e\Phi$. From these, one finds

$$\dot{\psi}=\nabla\psi\cdot\mathbf{v}_D=(c/e)\partial_{\alpha_p}V,\quad \dot{\alpha}_p=\nabla\alpha_p\cdot\mathbf{v}_D=-(c/e)\partial_\psi V, \tag{3}$$

which manifest a canonically conjugate structure. Making use of the bounce action $J(\psi,\alpha_p|\mu,E)\equiv(2\pi)^{-1}\oint dsMv_\parallel(s)$ (with s the arc length along a field line), one obtains bounce-averaged expressions for these:

$$\bar{\dot{\psi}}=-(c/e)\partial_{\alpha_p}J/\partial_E J=(c/e)\partial_{\alpha_p}H,$$
$$\bar{\dot{\alpha}}_p=(c/e)\partial_\psi J/\partial_E J=-(c/e)\partial_\psi H, \tag{4}$$

which also display the conjugate structure. (H is the Hamiltonian.) From these one may compute

$$\bar{\dot{r}}=(dr/d\psi)\bar{\dot{\psi}}\simeq(dr/d\psi)(c/e)\partial_\theta\bar{V},$$
$$\bar{\dot{\theta}}\simeq\bar{\dot{\alpha}}_p\simeq-(dr/d\psi)(c/e)\partial_r\bar{V}. \tag{5}$$

A. Optimization by reduction of $\bar{\dot{r}}$

In 1968 Palumbo pointed out[25] that if one could create a configuration having B a function of ψ only, $B=B(\psi)$, then [neglecting Φ in Eqs. (3)] $\dot{\psi}=0$. Such configurations are termed "isodynamic." However, toroidal isodynamic configurations do not exist, since these must have nonzero curvature $\boldsymbol{\kappa}(\zeta)=\kappa\hat{\boldsymbol{\kappa}}$ at some points along their magnetic axes, and at those places, B must have a cosinusoidal θ dependence,[26] $B\simeq B_x(1-\kappa x\cos(\theta))$, with $x=\psi^{1/2}x_1(\zeta)$ the distance from the axis to a point $\mathbf{x}$ on the flux surface ψ in the local major radial direction $\hat{\mathbf{R}}=-\hat{\boldsymbol{\kappa}}$.

A weaker version of this notion was advanced by Hall and McNamara,[27] investigating mirror equilibria. They found configurations for which $J=J(\psi)$, so that from Eq. (4), $\bar{\dot{\psi}}=0$. Such configurations are termed "omnigenous." In contrast to isodynamic configurations, examples of toroidal omnigenous configurations do exist. Indeed, for any symmetric system, where B depends on only one of the two angles parametrizing a flux surface, J will be a function of ψ alone, and thus have $\bar{\dot{\psi}}=0$. Thus, tokamaks and straight stellarators are omnigenous.

In 1983 Boozer noted[28] that if a system has a symmetry in flux coordinates, its particle orbits and transport are "isomorphic to" those of any other symmetric system, regardless of their appearance in real space. That is, the orbits and transport coefficients in one system may be gotten from those of the other by a simple parameter mapping between the two. This general observation set the stage for the discovery by Nührenberg and Zille[29] of the first QH configuration, a toroidal configuration approximately possessing the symmetry $B=B(\psi,\eta)$ in flux coordinates of a genuinely straight stellarator. This was followed some years later by the discovery by Nührenberg, *et al.*[30] and Garabedian[31] of QA configurations, approximately possessing the symmetry $B=B(\psi,\theta)$ of a tokamak, while being fully 3D in real space.

We sketch the means by which shaping can produce QA symmetry in a 3D stellarator. Consider an $m=2$ stellarator. At lowest order in an expansion about the magnetic axis, such a device has an elliptical cross section, which deforms as one moves in ζ (while keeping the same area, for flux conservation and ζ independence of B_x), and thus, the minor radial scale factor x_1 has a ζ dependence. If $\kappa(\zeta)$ is varied so that $\kappa(\zeta)x_1(\zeta)=$const, the above expression for B will also be independent of ζ, as desired. The maintenance of this ζ independence at higher order is complicated, but can be approximately achieved numerically in the automated optimization codes used to develop modern stellarator designs.

Another quasisymmetric (QS) system one might seek is one with QP symmetry, for which $B=B(\psi,\zeta)$, and with this as a goal, the QPS design has achieved excellent neoclassical confinement properties. However, due to the same cos θ dependence noted above for B in regions of nonzero $\kappa(\zeta)$, configurations having QP symmetry everywhere do not exist. Instead, in common with the W7X QO/QI design, the QPS device achieves good QP symmetry in low-field straight segments ($\kappa=0$), connected by higher-field, large-κ bends, where the θ dependence is appreciable. Thus, QPs are actually members of the QO/QI family of stellarators, to which we now turn.

In contrast to the concepts discussed to this point, a quasi-omnigenous (QO) or quasi-isodynamic (QI) device is *non*-symmetric, even in flux coordinates. (The terms QO and QI are equivalent, though the terms omnigenous and isodynamic are not, as discussed earlier.) Instead, it reduces $\bar{\dot{r}}$ by the near-cancellation of the usual δ_t term in Eq. (1) which yields $\bar{\dot{r}}$ by a second term, arising from the modulation $k(\mathbf{x})$ over a flux surface of ripple strength δ_h. The original QOs (Ref. 32) were members of the "σ configuration" family of model fields, for which k was approximately given by $k(\theta|\sigma)=(1-\sigma\cos\theta)$, and $c(\theta)=\cos\theta$. For $\sigma=0$, $\delta_h=\varepsilon_h$ has

the unmodulated form of a conventional stellarator [Fig. 1(c)], while for $\sigma>0$, the ripple is localized toward the inboard side of the torus, characteristic of QOs, such as in Fig. 1(e), and of "Meyer-Schmidt" (MS) configurations.[33] Those earlier nontransport-optimized configurations sought to minimize the equilibrium shift at higher β by reducing the Pfirsch-Schlüter currents. This was achieved by localizing δ_h toward $\theta=\pi$ in such a way that the δ_t term in Eq. (1) was approximately eliminated. For QOs, the δ_t term must *not* be eliminated; it is the balance between it and the δ_h contribution which reduces $\bar{\dot{r}}$. A first concrete realization of the QO/QI approach was given in the first "helias" configuration,[34] a forerunner of the W7X design.

Using Eq. (1) in (5), one finds $\bar{\dot{r}}\simeq -v_{B0}[\partial_\theta\delta_t+(\partial_\theta\delta_h)\overline{\cos\eta}]=v_{B0}\sin\theta(\varepsilon_t-\sigma\varepsilon_h\cos\eta)$, where the second form specializes the first to the σ model. Here, $\overline{\cos\eta}$ is the bounce average of $\cos\eta$, and we have used the fact that $\overline{\sin\eta}\simeq 0$. The two terms contributing are apparent in both forms. For $\sigma p\cos\eta=1$, one sees that the new, second term in the second form cancels the conventional first term ($\propto\varepsilon_t$). However, $\overline{\cos\eta}$ depends upon the well-depth parameter $y\equiv[W/\mu\bar{B}-1+\varepsilon_t c(\theta)+\delta_h]/(2\delta_h)$, equal to 0 for particles most deeply ripple trapped and 1 for those marginally trapped. Thus, this cancellation will only hold for particles with a single y. This is the "quasi" aspect of "quasi-omnigenous." One chooses σp so that $\bar{\dot{r}}=0$ for particles with y in the most troublesome range, namely deeply trapped particles, for which $\overline{\cos\eta}(y)=2E(y^{1/2})/K(y^{1/2})-1\lesssim 1$. (Here, K and E are the complete elliptic integrals.) Near that y, while not precisely 0, $\bar{\dot{r}}$ is still small, which is adequate to reduce the overall $D\sim\langle\bar{\dot{r}}^2\rangle$ by a factor of 10–30.[32]

We note that QO configurations can continuously approach QH ones, which are genuinely omnigenous, by having $\sigma\to 0$ while $p\to\infty$ in such a way that $\sigma p=$const. Thus, the QO subspace extends the QH subspace of transport-optimized configurations, by relaxing the requirement of full omnigenity.

Other interesting extensions of the transport optimized concepts discussed thus far have also been discovered. One is the "isometric,"[35] or "approximately omnigenous"[36] concept. For these, requiring that $J\simeq J(\psi)$ for *almost all* particles results in the "isometry condition," that the length along **B** between any two contours with constant $B=|\mathbf{B}|$ is a constant (i.e., independent of α_p). This is trivially satisfied for symmetric configurations, but remarkably, nonsymmetric configurations exist which also approximately satisfy it. Interestingly, while particles accordingly have $\bar{\dot{\psi}}=0$, their banana widths and shapes vary with α_p. Another extension is the "pseudosymmetric" family of configurations.[37] For these, only sufficient closeness to a quasisymmetry is required that the ripple wells along field lines are eliminated. In achieving this, the sb mechanism, usually dominant, is eliminated, leaving only the less problematic bd mechanism. To our knowledge, no experimental implementations of these extensions have yet been designed, presumably because the transport reductions achieved with the other concepts already appears adequate.

B. Optimization by enhancement of Ω_θ

In steady-state, a toroidal magnetic confinement system must satisfy the "ambipolarity constraint"

$$0=\sum_s e_s\Gamma_s, \tag{6}$$

so that the system does not continue to charge, changing $E_r(r)$. The symmetric-branch contributions to these fluxes are "intrinsically ambipolar," i.e., satisy Eq. (6) independent of $E_r(r)$, a property stemming from conservation under collisions of the momentum conjugate to the symmetry direction. The nonsymmetric transport channels derive instead from momentum exchange between particles and the magnetic field of the system itself, and so are not intrinsically ambipolar. Thus, if the ion and electron fluxes initially differ, E_r will change until condition (6) is satisfied. Neglecting in addition to the bd contribution, the full fluxes in Eq. (6) may be replaced by the sb fluxes, expressions for which were given in Sec. III. One notes that E_r enters Eq. (2) in two places, through the thermal-force term $[n_s'/n_s+\ldots]$, and through the diffusion coefficients D_q.

If the plasma initially has $E_r=0$, both ions and electrons will be in the $1/\nu$ regime, so that, since $D_{-1i}/D_{-1e}\sim M_i^{1/2}/M_e^{1/2}\gg 1$ for $T_i\sim T_e$, the ions will leave the system more quickly, producing a negative E_r, increasing in size until (6) is satisfied, with the ions in the ν^1 or $\nu^{1/2}$ regime. This root, called the "ion root" E_{ri}, was the first solution of Eq. (6) discovered.[18] Subsequently, it was recognized that multiple roots of this condition exist.[38] Keeping only the sb branch contributions, it was found that there are two additional roots to Eq. (6). (See Ref. 38 for a diagrammatic means of understanding this.) When parameters are such that all three roots are real, the two new roots are an intermediate one, E_{r0}, unstable to fluctuations in E_r, and a second stable root, called the "electron root" E_{re}, positive and typically large compared with $|E_{ri}|$, in which the ions hold in the electrons. For $T_i\sim T_e$, both Γ_s and Q_s are typically much smaller than at E_{ri}, thereby reducing transport via electrostatically enhancing Ω_θ.

The electron root has been observed experimentally on several machines[39–41] using electron cyclotron heating (ECH), and on LHD (Ref. 42) using neutral beam injection NBI heating. The ECH experiments achieved E_{re} by producing elevated electron transport, thereby removing the potential advantage of the root. The NBI experiment accessed E_{re} with $T_e\sim T_i$, and improved confinement of both species was observed.

The values of the roots $E_{r,a=i,0,e}$ of (6) depend upon plasma profiles such as density and temperature, which vary with radius r and time t. These profiles in 3D systems thus provide extra "knobs" not present in AS systems, giving one control over the $E_r(r)$ profile, and the resultant plasma flows. Note that controlling E_r in this way does not require strong ripple; the nonsymmetric fluxes may be small compared with the symmetric nc or the turbulent ones.

Condition (6) is radially local, providing a set of roots E_{ra} at each r and time t, but is insufficient to describe what happens when there is a jump between roots at two neigh-

boring radii, or when E_r is not at one of the roots, so that the system is evolving in time. A partial differential equation for $E(r,t)$ is required for this. Such a partial differential equation was developed in Refs. 43 and 44, of the form

$$\partial_t[C_E E_r] = (V')^{-1}\partial_r(V' D_E \partial_r E_r) + \sum_s e_s \Gamma_s,$$

with C_E a constant, and D_E the "electric diffusion coefficient," which determines the scale over which root jumps take place. In steady state and away from radii where root-jumping occurs, only the final term survives, recovering Eq. (6). We return to root-jumping in Sec. V.

The discussion thus far has been concerned mainly with the transport of thermal particles, but the confinement of energetic ions, such as neutral beam or α particles, is of course another important confinement constraint. Some design features which improve thermal confinement, notably the reduction of $\bar{\dot{r}}$, will also tend to improve energetic particle confinement. However, there are some important differences between thermal and energetic confinement so that, for example, NCSX has much lower $1/\nu$ transport than W7X, but a reactor-size W7X has much better α confinement than NCSX. (This is not a generic difference between QAs and QOs. For example, in the ARIES-CS QA reactor design, a descendant of NCSX, the α confinement approaches that of W7X.[45] The properties of these systems are still evolving.) One difference is that energetic particles are highly insensitive to the electrostatic potential Φ. Thus, the form of their orbits is determined entirely by the structure of $B(\mathbf{x})$. Also, energetic ions are almost collisionless, so the full form of their collisionless trajectories is essential to their confinement characteristics. Thus, enhancement of $\Omega_{\theta E}$ is of no use for energetic confinement, and devices must be designed to provide a magnetic counterpart $\Omega_{\theta B} \propto \partial_r B$ in its place. Thus, for example, the alpha loss fraction in a reactor-size W7X improves dramatically[46] as β is raised from 0 to 4%, as the plasma digs a magnetic well, enhancing $\Omega_{\theta B}$.

V. OPTIMIZATION OF TURBULENT TRANSPORT

The approaches discussed up to now can reduce nc transport to levels below that of turbulent transport, so in recent years, reducing turbulent transport has also become of interest.

In tokamaks, internal transport barriers (ITBs) have been produced, in which a strong flow shear[47] suppresses the microturbulence, and stellarators with adequate quasisymmetry may be able to induce ITBs in similar fashion. Additionally, however, the nonsymmetric transport channels in stellarators provide a means for producing the requisite shear in E_r and resultant flow-shear not available to tokamaks, e.g., from jumps between the ion and electron roots. Such root-jump-induced ITBs have been experimentally observed on W7AS,[48] LHD,[49] and on CHS.[50]

A second, more general strategy for mitigating turbulent transport is by controlling the shaping of the device. While tokamaks and stellarators conform to quite similar empirical transport scaling laws,[51] the normalization factor multiplying the energy confinement time τ_E is device-dependent.[52] This may be expected, since a stellarator's shape determines factors which strongly influence the microstability of the device, such as global and local shear, locations of good and bad curvature, locations of trapped particles, as well as its equilibrium flows, and these will affect the character of the turbulence the device supports. Interestingly, those devices which have some neoclassical optimization, such as W7AS and the inward-shifted LHD, also tend to have lower anomalous transport.[52] Recent work on this[53,54] suggests this correlation is not coincidental, arguing that lower nc transport implies smaller in-surface viscosities, implying less damping of zonal flows, and thus stronger suppression by them of the turbulence.

Another mechanism by which shaping may be able to reduce anomalous transport is described in Ref. 55. There, it is shown that a turbulent spectrum can provide an anomalous increment ν_{an} to the collisional particle pitch-angle scattering, $\nu_{ef} = \nu + \nu_{an}$. As confirmed by guiding-center simulations, for particles in a neoclassical regime (such the $1/\nu$ regime) where diffusion falls with increasing ν, this increment can *reduce*, rather than enhance, overall radial transport, contrary to our usual tokamak-based intuitions. The size of this effect depends upon the structure of the modes comprising the spectrum, which in turn depends upon the plasma shape.

VI. DISCUSSION

The evolution of many of the nc concepts described here may be seen as an effort to enlarge the space of earlier optimized configurations, by relaxing an optimization principle while not sacrificing too much in transport. For example, the space of toroidal isodynamic configurations is null, properly contained within the non-null space of toroidal omnigenous configurations. Weakening the real-space symmetry required for omnigenous configurations to only approximate symmetry in flux coordinates further enlarges the space to QS configurations. And requiring $\bar{\dot{r}}=0$ for only the most troublesome particles further extends the QS space to that of QOs. For each of the three general nc mitigation approaches, viz., QS, QO/QI, and Ω_θ enhancement, experiment already indicates that the technique is helpful—for the QS approach, on the HSX stellarator, for the QO approach, on LHD and CHS in their inward-shifted configurations, and for Ω_θ enhancement, on a range of stellarators, both optimized and not. Further test and refinement of these methods will be possible as new experiments implementing them become operational. The set of nc mitigation approaches which have been discussed permit reducing stellarator thermal nc transport to levels where it is subdominant to turbulent transport over the full plasma column for typical operating temperatures. At the same time, the nonintrinsic ambipolarity of the nonsymmetric fluxes, even when small compared with the turbulent ones, gives stellarators added control over the E_r profile, helpful for control of the plasma flow and turbulent transport.

The development of turbulent mitigation methods is now in its early stages, perhaps analogous to the situation for nc mitigation in the early 1980s. As then, the numerical tools needed to effectively study the effects on transport of differ-

ent stellarator designs are now becoming available, currently including linear stability, nonlinear simulation, and optimizer codes valid for stellarators. Explorations using these tools should provide a growing list of techniques for turbulent optimization.

ACKNOWLEDGMENTS

The author is grateful to A. Boozer, S. Gerhardt, L.-P. Ku, D. Mikkelsen, G. Rewoldt, D. Spong, and J. Talmadge for useful discussions.

This work supported by the U. S. Department of Energy Contract No. DE-AC02-76-CHO3073.

[1] M. Fujiwara, Y. Takeiri, T. Shimozuma *et al.*, Nucl. Fusion **40**, 1157 (2000).
[2] C. Beidler, G. Grieger, F. Herrnegger, E. Harmeyer, J. Kisslinger, W. Lotz, H. Maassberg, P. Merkel, J. Nuhrenberg, F. Rau, J. Sapper, F. Sardei, R. Scardovelli, A. Schluter, and H. Wobig, Fusion Technol. **17**, 148 (1990).
[3] J. N. Talmadge, V. Sakaguchi, F. S. B. Anderson, D. T. Anderson, and A. F. Almagri, Phys. Plasmas **8**, 5165 (2001).
[4] G. H. Neilson, M. C. Zarnstorff, J. F. Lyon, and the NCSX Team, J. Plasma Fusion Res. **78**, 214 (2002).
[5] D. A. Spong, S. P. Hirshman, L. A. Berry *et al.*, Nucl. Fusion **41**, 711 (2001).
[6] A. H. Boozer, Phys. Fluids **23**, 904 (1980).
[7] T. S. Pedersen, A. H. Boozer, J. P. Kremer, R. Lefrancois, F. Dahlgren, N. Pomphrey, W. Reiersen, and W. Dorland, Fusion Sci. Technol. **46**, 200 (2004).
[8] S. Murakami, A. Wakasa, H. Maassberg, C. D. Beidler, H. Yamada, K. Y. Watanabe, and LHD Experimental Group, Nucl. Fusion **42**, L19 (2002).
[9] F. L. Hinton and R. D. Hazeltine, Rev. Mod. Phys. **48**, 239 (1976).
[10] S. P. Hirshman and D. J. Sigmar, Nucl. Fusion **21**, 1079 (1981).
[11] P. Helander and D. J. Sigmar, *Collisional Transport in Magnetized Plasmas* (Cambridge University Press, Cambridge, 2002).
[12] A. A. Galeev and R. Z. Sagdeev, *Reviews of Plasma Physics*, edited by M. A. Leontovich (Consultants Bureau, New York, 1979), Vol. 7, p. 257.
[13] L. M. Kovrizhnykh, Phys. Scr. **43**, 194 (1984).
[14] A. Pytte and A. H. Boozer, Phys. Fluids **24**, 88 (1981).
[15] A. H. Boozer, Phys. Fluids **23**, 2283 (1980).
[16] R. J. Goldston, R. B. White, and A. H. Boozer, Phys. Rev. Lett. **47**, 647 (1981).
[17] R. Linsker and A. H. Boozer, Phys. Fluids **25**, 143 (1982).
[18] A. A. Galeev, R. Z. Sagdeev, H. P. Furth, and M. N. Rosenbluth, Phys. Rev. Lett. **22**, 511 (1969).
[19] A. A. Galeev and R. Z. Sagdeev, Sov. Phys. Usp. **12**, 810 (1970).
[20] A. A. Galeev, R. Z. Sagdeev, and H. P. Furth, Zh. Prikl. Mekh. Tekh. Fiz. 3 (1968).
[21] A. Gibson and D. W. Mason, Plasma Phys. **11**, 121 (1969).
[22] T. E. Stringer, Nucl. Fusion **12**, 689 (1972).
[23] J. W. Connor and R. J. Hastie, Phys. Fluids **17**, 114 (1974).
[24] H. E. Mynick, Phys. Fluids **26**, 2609 (1983).
[25] D. Palumbo, Nuovo Cimento B **53**, 507 (1968).
[26] D. A. Garren and A. H. Boozer, Phys. Fluids B **3**, 2805 (1991).
[27] L. S. Hall and B. McNamara, Phys. Fluids **18**, 552 (1975).
[28] A. H. Boozer, Phys. Fluids **26**, 496 (1983).
[29] J. Nührenberg and R. Zille, Phys. Lett. A **129**, 113 (1988).
[30] J. Nührenberg, W. Lotz, and S. Gori, in *Theory of Fusion Plasmas*, edited by E. Sindoni, F. Tryon, and J. Vaclavik (SIF, Bologna, 1994).
[31] P. R. Garabedian, Phys. Plasmas **3**, 2483 (1996).
[32] H. E. Mynick, T. K. Chu, and A. H. Boozer, Phys. Rev. Lett. **48**, 322 (1982).
[33] F. Meyer and H. U. Schmidt, Z. Naturforsch. A **13A**, 1005 (1958).
[34] J. Nührenberg and R. Zille, Phys. Lett. **114A**, 129 (1986).
[35] A. A. Skovoroda and V. D. Shafranov, Plasma Phys. Rep. **21**, 886 (1995).
[36] J. R. Cary and S. G. Shasharina, Phys. Rev. Lett. **78**, 674 (1997).
[37] M. I. Mikhailov, V. D. Shafranov, and D. Suender, Plasma Phys. Rep. **24**, 653 (1998).
[38] H. E. Mynick and W. N. G. Hitchon, Nucl. Fusion **23**, 1053 (1983).
[39] H. Idei, K. Ida, H. Sanuki *et al.*, Phys. Rev. Lett. **71**, 2220 (1993).
[40] H. Maassberg, C. D. Beider, U. Gasparino, M. Romé, and the W7-AS Team, Phys. Plasmas **7**, 295 (2000).
[41] F. Castejon, V. Tribaldos, I. Garcia-Cortes, E. de la Luna, J. Herranz, I. Pastor, T. Estrada, and the TJ-II Team, Nucl. Fusion **42**, 271 (2002).
[42] K. Ida, H. Funaba, S. Kado, K. Narihara, K. Tanaka, Y. Takeiri, Y. Nakamura, N. Ohyabu, K. Yamazaki, M. Yokoyama *et al.*, Phys. Rev. Lett. **86**, 5297 (2001).
[43] K. C. Shaing, Phys. Fluids **27**, 1567 (1984).
[44] D. E. Hastings, W. A. Houlberg, and K. C. Shaing, Nucl. Fusion **25**, 445 (1985).
[45] L. P. Ku and P. Garabedian, Proceedings of the 15th International Stellarator Workshop, Madrid, Spain, 2005, to be published in Fusion Sci. Technol.
[46] W. Lotz, P. Merkel, J. Nührenberg, and E. Stumberger, Plasma Phys. Controlled Fusion **34**, 1037 (1992).
[47] T. S. Hahm and K. H. Burrell, Phys. Plasmas **2**, 1648 (1995).
[48] U. Stroth, K. Itoh, S.-I. Itoh, H. Hartfuss, H. Laqua, the ECRH team, and the W7-AS team, Phys. Rev. Lett. **86**, 5910 (2001).
[49] K. Ida, T. Shimozuma, H. Funaba *et al.*, Phys. Rev. Lett. **91**, 085003 (2003).
[50] T. Minami, A. Fujisawa, H. Iguchi *et al.*, Nucl. Fusion **44**, 342 (2004).
[51] U. Stroth, Plasma Phys. Controlled Fusion **40**, 9 (1998).
[52] H. Yamada, J. H. Harris, A. Dinklage, E. Escasibar, F. Sano, S. Okamura, U. Stroth, A. Kus, J. Talmadge, S. Murakami, M. Yokoyama, C. Beidler, V. Tribaldos, and K. Y. Watanabe, Proceedings of the 31st EPS Conference on Plasma Physics, P5-9, London, June 29-July 2, 2004.
[53] H. Sugama and T. H. Watanabe, Phys. Rev. Lett. **94**, 115001 (2005).
[54] K. C. Shaing, Phys. Plasmas **12**, 082508 (2005).
[55] H. E. Mynick and A. H. Boozer, Phys. Plasmas **12**, 062513 (2005).